**EUROPEAN ORGANIZATION FOR NUCLEAR RESEARCH**

**Letter of Intent to the ISOLDE and Neutron Time-of-Flight Committee**

# $\gamma$-ray production by high energy neutrons in water

January 10, 2024

M. Bacak[1], N. Bhuiyan[2,3], M. Birch[4], M. Boromiza[5], A. Casanovas[6], C. Cazzaniga[2], N. Colonna[7], A. Gandhi[5], F. Garcia Infantes[1,8], T. Katori[3], Y. Koshio[9], G. Lorusso[10], A. Mengoni[11,12], F. Nakanishi[9], A. Negret[5], N. Patronis[1,13], C. Petrone[5], T. Tano[9], T. Wright[4] and the n_TOF Collaboration[14]

[1] *European Organization for Nuclear Research (CERN), Switzerland*
[2] *ISIS Neutron Source, United Kingdom*
[3] *King's College London, United Kingdom*
[4] *University of Manchester, United Kingdom*
[5] *Horia Hulubei National Institute for R&D in Physics and Nuclear Engineering, Romania*
[6] *Universitat Politècnica de Catalunya, Spain*
[7] *Istituto Nazionale di Fisica Nucleare, Sezione di Bari, Italy*
[8] *University of Granada, Spain*
[9] *Okayama University, Japan*
[10] *National Physical Laboratory London, United Kingdom*
[11] *Agenzia nazionale per le nuove tecnologie (ENEA), Italy*
[12] *Istituto Nazionale di Fisica Nucleare, Sezione di Bologna, Italy*
[13] *University of Ioannina, Greece*
[14] *www.cern.ch/n_TOF*

**Spokesperson:** N. Bhuiyan (nahid.bhuiyan@stfc.ac.uk), M. Bacak (michael.bacak@cern.ch)
**Technical coordinator:** O. Aberle (oliver.aberle@cern.ch)

CERN-INTC-2024-009 / INTC-I-269
10/01/2024

**Abstract:**

In Super-Kamiokande, the $\gamma$-rays induced from neutron-oxygen reactions result in a considerable background in various sensitive searches. As there is a lack of neutron cross section data beyond a few tens of MeV for oxygen, the interaction models contribute towards a large uncertainty and thereby limit sensitivity. In order to provide the required information we propose to measure the $\gamma$-rays produced by the interaction of high energy neutrons up to 200 MeV in a water target with $LaBr_3$ detectors at n_TOF EAR1. The induced $\gamma$-ray spectra will be recorded as a function of neutron energy. This kind of information cannot be retrieved from previous publications or can only be compared to other experimental data in limited energy intervals below 20 MeV and at 80 MeV.

**Requested protons:** $3 \cdot 10^{17}$ in EAR1 and $3 \cdot 10^{18}$ in EAR1 neutron escape line (NEL)
**Experimental Area:** EAR1 and EAR1 NEL

# 1 Introduction & Motivation

Super-Kamiokande (Super-K) is a Water-Cherenkov detector located in Japan, primarily utilised for studying neutrinos. Understanding the propagation of neutrino interaction products within the water media is crucial to identify signals and backgrounds, and neutron tagging has been implemented in 2008 to aid identification [1], with further enhancements in 2020 with the addition of gadolinium [2].
In particular, neutron tagging strengthens the identification of inverse-beta decay (IBD) events, illustrated in Fig. 1 (left), $\bar{\nu}_e + \mathrm{p} \rightarrow e^+ + \mathrm{n}$, which is the signal for neutrinos in the MeV-scale [3]. Here, the detected light from the primary positron and the delayed neutron capture are correlated, thereby eliminating many backgrounds. However, the major remaining background is the neutral current quasi-elastic (NCQE) interactions from atmospheric neutrinos, $\nu(\bar{\nu}) + {}^{16}\mathrm{O} \rightarrow \nu(\bar{\nu}) + {}^{15}\mathrm{O} + \gamma + \mathrm{n}$ or $\nu(\bar{\nu}) + {}^{16}\mathrm{O} \rightarrow \nu(\bar{\nu}) + {}^{15}\mathrm{N} + \gamma + \mathrm{p}$, illustrated in Fig. 1 (right).

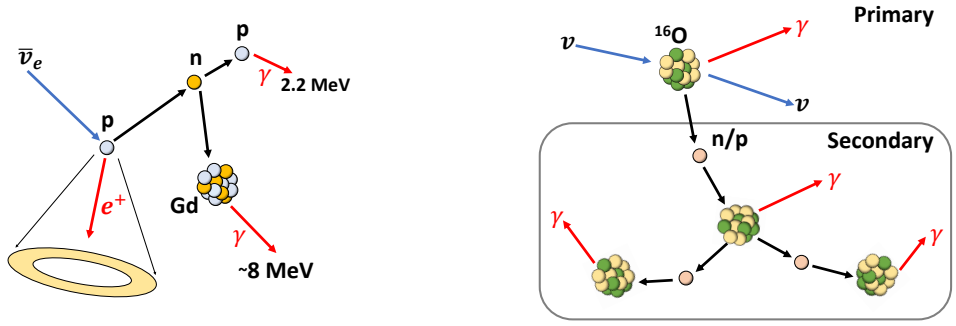


Figure 1: Representation of IBD (left) and NCQE (right) interactions as seen in Super-K.

Here, an energetic atmospheric neutrino interacts with oxygen nuclei without charge exchange. The T2K and Super-K experiments reported the NCQE cross section based on the primary $\gamma$-rays from the nuclear de-excitation [4, 5, 6, 7], however, with large uncertainties due to the subsequent interactions by the liberated nucleons.
These nucleons have energies ranging from a few to a few hundreds of MeV, and can re-interact on oxygen nuclei to produce secondary $\gamma$-rays through various processes within $\mathcal{O}(100\,\mathrm{ns})$, with examples listed in Tab. 1. These $\gamma$-rays are collectively reconstructed as part of a primary Cherenkov signal. The liberated nucleons can also survive consecutive secondary interactions such that they also produce $\gamma$-rays in the time range used to search for delayed signals. In this way, NCQE interactions can imitate both components of an IBD signal and therefore survive as a background. Simulations are used to estimate the amount of wrongly assigned NCQE reactions as IBD signals (i.e. background). The relevant inelastic neutron-oxygen cross sections are only measured and evaluated up to 30 MeV. Moreover, GEANT4 uses these libraries up to 20 MeV before transitioning into nuclear cascade models such as INCL, BERT and BIC [8]. Consequently, the secondary

| Energy | Parent ($J^\pi$) | Physics process |
|---|---|---|
| 7.12 MeV | $^{16}$O($1^-$) | $^{16}\mathrm{O}(n,n')^{16}\mathrm{O}^*$ |
| 6.92 MeV | $^{16}$O($2^+$) | $^{16}\mathrm{O}(n,n')^{16}\mathrm{O}^*$ |
| 6.32 MeV | $^{15}$N($\frac{3}{2}^-$) | $^{16}\mathrm{O}(n,np)^{15}\mathrm{N}^*$ |
| 6.13 MeV | $^{16}$O($3^-$) | $^{16}\mathrm{O}(n,n')^{16}\mathrm{O}^*$ |
| 5.27 MeV | $^{15}$N($\frac{5}{2}^+$) | $^{16}\mathrm{O}(n,n')^{16}\mathrm{O}^*$ then $^{16}\mathrm{O}^* \rightarrow ^{15}\mathrm{N}^* + p$, or $^{16}\mathrm{O}(n,np)^{15}\mathrm{N}^*$ |
| 4.44 MeV | $^{12}$C($2^+$) | $^{16}\mathrm{O}(n,n')^{16}\mathrm{O}^*$ then $^{16}\mathrm{O}^* \rightarrow ^{12}\mathrm{C}^* + \alpha$, or $^{16}\mathrm{O}(n,n\alpha)^{12}\mathrm{C}^*$ |
| 3.68 MeV | $^{13}$C($\frac{3}{2}^-$) | $^{16}\mathrm{O}(n,\alpha)^{13}\mathrm{C}^*$ |
| 2.31 MeV | $^{14}$N($0^+$) | $^{16}\mathrm{O}(n,2np)^{14}\mathrm{N}^*$ |
| 2.30 MeV | $^{15}$N($\frac{7}{2}^+$) | $^{16}\mathrm{O}(n,np)^{15}\mathrm{N}^*$ |

Table 1: Examples of $\gamma$-rays' energies of interest alongside their parent nuclei and physics processes. The detector's response templates to these $\gamma$-rays were sufficient to fit the data in E487 at RCNP as shown in Fig. 2. De-excitation of other levels might contribute to the measured spectra, e.g. the cascades depopulating the 8.87 MeV $2^-$ state of $^{16}$O.

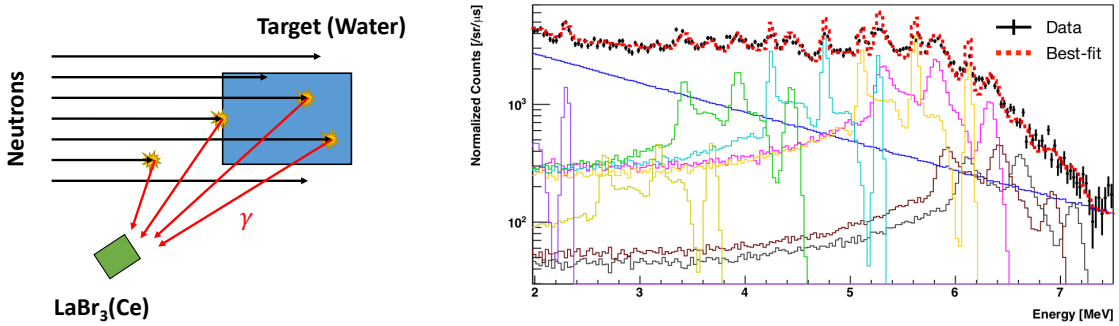


Figure 2: Schematic illustration of experiment E487 at RCNP (left). Measured spectra with best-fit of signal templates for the $\gamma$-rays observed as listed in Tab. 1 (right) [10].

interaction models are associated with large systematic uncertainties and lead to different results based on the model used [7]. This lack of data thereby limits the sensitivity of various searches, including supernovae relic neutrinos, sterile neutrinos and dark matter. To improve this, experiment E487 at RCNP aimed to study neutron-oxygen interactions in the neutron energy regime above 30 MeV [9]. This used a quasi-monoenergetic 80 MeV neutron beam on a cylindrical acrylic vessel, 20.0 cm in diameter and 26.5 cm in height, as schematically illustrated in Fig. 2 (left).

The experiment measured the prompt $\gamma$ spectra using a lead shielded $LaBr_3$ scintillator. The RCNP data was reconstructed by simultaneously fitting the simulated detector responses of the individual $\gamma$-rays listed in Tab. 1, thereby inferring the $\gamma$ production cross sections at 80 MeV neutron energy [10].

To implement such results into models, a full spectrum of the production cross sections up to 200 MeV range is necessary. Furthermore, it is also of interest to cross check the results of E487 given the complexity of working with neutrons in this energy regime. We therefore would like to propose a similar experiment at n_TOF and use a time-of-flight technique to simultaneously measure these $\gamma$ yields from neutron-oxygen reactions with

the emphasis on the neutron energy range from 10 to 200 MeV. Therein the sufficient bin size is between 10 to 20 MeV for the intended purpose. These $\gamma$ yields are the direct consequence of the high energy neutron-oxygen inelastic cross sections, and therefore the data would be sufficient for improving the gamma emission models used in simulations. Estimates show [11] that the systematic error in the evaluation of NCQE interactions due to uncertainties in secondary $\gamma$ productions amounts to 13% of its total 20% systematic error. As such, the $\gamma$ yield data can improve the estimations of wrongly assigned NCQE interactions in IBD and thereby increase the sensitivity of various searches in both Super-K and the upcoming Hyper-K. Moreover, these measurements can also be beneficial to other neutrino experiments using water-based detector media, as well as pioneer a method for studying high energy neutron interactions.

## 2 Challenge & Feasibility

Following and extending the recent efforts on the development of $LaBr_3$ detectors for MeV neutron energy $\gamma$-ray spectroscopy at n_TOF [12] these detectors have shown promising first results and seem suited for this experiment as we explain in the following.
The first requirement is a stable detector response shortly after the $\gamma$-flash at 200 MeV neutron energy. To estimate the reliability of the detector response, we looked at the signal shape (FWHM and rise time) from 2023 data taken in a parasitic experiment in EAR1 at approx. 184 m flight path. A 2"x1.5" $LaBr_3$ detector was used to record the inelastic neutron scattering $\gamma$-rays from a 1 mm thick $^{56}$Fe sample with 20 mm diameter. The detector was placed at a distance of 11 cm and a backwards angle of 125°. The crystal size, the close distance to the sample and the significant amount of sample mass (2.3 g and higher Z than water) are realistic conditions for the proposed experiment. In the left panel of Fig. 3 the FWHM of this detector's signals are displayed as a function of time-of-flight (TOF). After the $\gamma$-flash at TOF=614 ns, the detector recovers and exhibits a stable signal shape behaviour at a TOF of 1 µs corresponding to a neutron energy of 250 MeV. The signals outside the main bands are due to pile-up and can be resolved by reducing the count rate (the count rate at 250 MeV/1 µs was approx. 1 MHz). The rise time (not shown) exhibits similar characteristics like the FWHM.

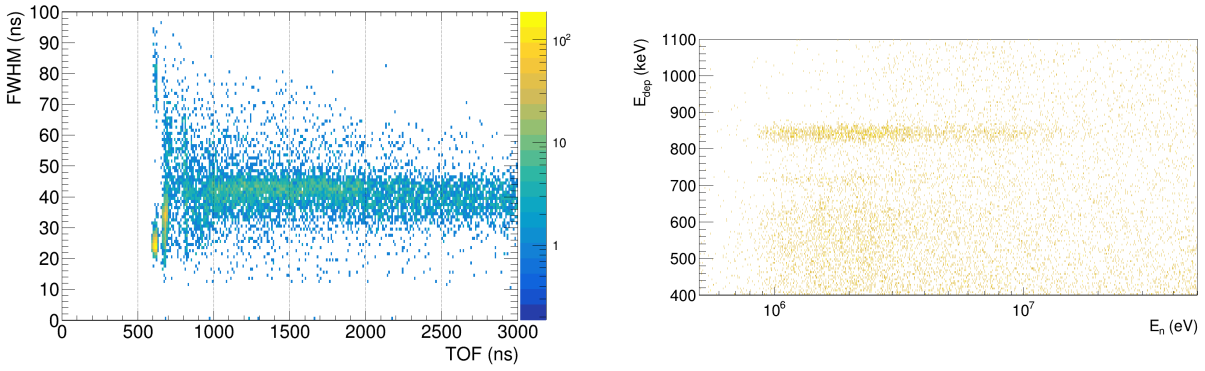


Figure 3: FWHM of reconstructed $LaBr_3$ detector signals at as a function of time-of-flight (left). Deposited energy in a $LaBr_3$ detector as a function of neutron energy (right).

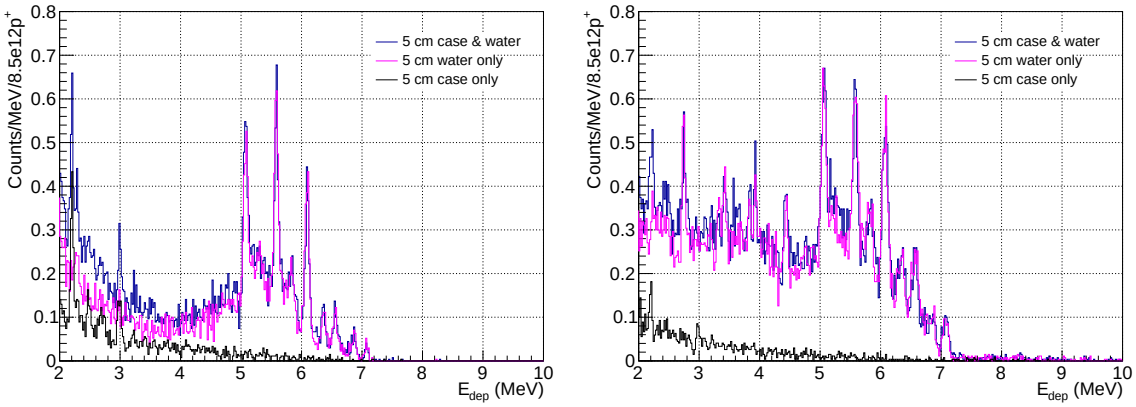


Figure 4: Simulated response of a 1.5"x1.5" detector at 20 cm detector-target distance in a neutron energy interval of 5-10 MeV (left) and 10-20 MeV (right).

The right panel of Fig. 3 shows that in the low MeV region we can cleanly identify the inelastic $^{56}$Fe(n,n')L1 line at 846 keV with an energy resolution of 3 %. Beyond 20 MeV the statistics decrease due to the involved cross section and a dip in the EAR1 neutron flux. For the purpose of studying these detector's gain stability at short TOFs we require beam time with a realistic water target due to potential beam induced ($\gamma$-flash) effects. Secondly, large pile-up corrections are to be avoided as they deteriorate the energy resolution of the measurement. Hence, the instantaneous count rates have been calculated via Monte Carlo simulations using the GEANT4 toolkit [8, 13] and the measured EAR1 neutron flux and beam profile. The water target has a diameter of 5 cm and is encapsulated in a 1 mm thick aluminium case. Different target thicknesses and detector-target distances have been considered to optimize the instantaneous count rate and maximizing statistics. Up to 20 MeV GEANT4 uses tabulated neutron cross sections, hence the 5-7 MeV $\gamma$-lines of oxygen (see Tab. 1) can be observed quite well as shown in Fig. 4. Above, the QGSP_INCLXX_HP physics list was used to estimate the production of any kind of $\gamma$-rays.
The instantaneous count rates per nanosecond for different detector and target configurations are shown in Fig. 5 considering all $\gamma$-rays with an energy above 100 keV. A rough estimation of a pile-up correction is shown in the right panel of Fig. 5 using the non-paralyzable model [14] with the detectors FWHM of 50 ns as time constant. The correction stays within reasonable limits (10 %) and using other dead time/pile-up models [15] will further improve the situation. Moreover, in order to reduce the count rate induced by low energy $\gamma$-rays, we intend to test several lead shielding configurations for the detectors. Beam time in the NEL will allow us to investigate the reliability of our count rate estimates compared to our chosen nuclear cascade model. Furthermore, dedicated and parasitic beam time in EAR1 and NEL respectively will allow us to get an idea of the signal-to-background ratio which is hard to infer from simulations as they are performed in a rather sterile environment, e.g. reliable modelling of the background induced by neutron scattering is nearly impossible.
Lastly, a solid $\gamma$-ray energy calibration and efficiency determination of the detectors up

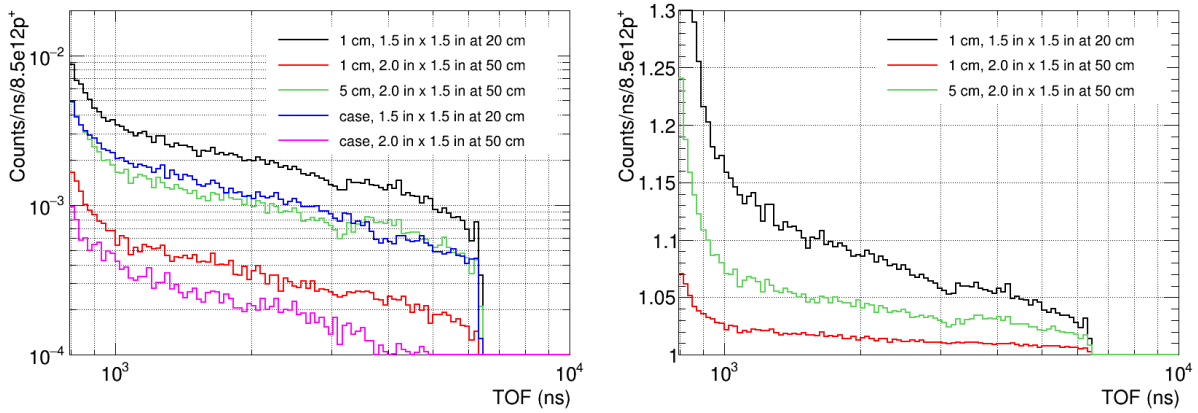


Figure 5: Average instantaneous count rates for different water thickness and detector configurations (left) and corresponding pile-up corrections (right).

to 10 MeV is required. Up to 6.13 MeV standard calibration sources will be used. For higher energies we intend to use neutron capture reactions [16] on $^{63}$Cu(n,$\gamma$) (7916.3 keV, $I_\gamma = 27.2\,\%$) and $^{58}$Ni(n,$\gamma$) (8998.4 keV, $I_\gamma = 35\,\%$) directly with the EAR1 beam. While we see no reason for failure, we lack experience with this method. Hence, parasitic beam time at NEL would allow testing the method for energy calibrations via (n,$\gamma$) reactions.

# 3 Summary and proton request

The systematic uncertainty and sensitivity of neutrino experiments based on water Cherenkov detectors is directly affected by the knowledge of the $\gamma$-ray production of high energy neutrons in water and specifically oxygen. There is almost no data beyond 30 MeV neutron energy for inelastic reactions on oxygen as such measurements are posing a challenge for instrumentation, and depending on the required neutron energy range, only a handful facilities around the world are available. n_TOF EAR1 provides neutrons up to several 100 MeV neutron energy and this physics case presents a clear motivation to follow and extend the ongoing efforts at n_TOF to develop a setup for $\gamma$-ray production measurements at high neutron energies.

In order to address open technical questions regarding our $LaBr_3$ setup discussed in section 2, we propose an optimization study which can be largely realized in EAR1's neutron escape line (NEL). We therefore request a total of $3 \cdot 10^{18}$ p$^+$ at the NEL to carry out the setup optimization with respect to detector gain stability investigations at very short TOFs, instantaneous count rate studies with and without lead shielding as well as a proof-of-principle for the (n,$\gamma$) energy calibration method. In order to study the effect of scattering and subsequent reactions (i.e. moderation effects) we intend to use several target thicknesses, namely 1, 5 and 25 cm of water. The beam time at the NEL is fully parasitic to the main experiment in EAR1 and can therefore be carried out in parallel.

In addition to answering the technical question we further request $3{\cdot}10^{17}$ dedicated protons in EAR1 to assess the signal-to-background conditions. This request is based on the current experimental knowledge and simulations of unshielded detectors in reasonable instan-

taneous counting rate conditions. In such conditions we expect 50-70 counts/day/detector in the main oxygen peak integrals in a neutron energy interval of 10-20 MeV, which we expect to be sufficient for judging the SBR and comparing to the NEL.
If the outcome of the measurements described in this LoI provides sufficient evidence for the feasibility of such an experiment a physics proposal for a dedicated measurement in EAR1 will be submitted in the future.

**Summary of requested protons:** $3.0 \cdot 10^{17}$ in EAR1 and $3.0 \cdot 10^{18}$ in EAR1 NEL

# References


[1] H. Watanabe et al. "First study of neutron tagging with a water Cherenkov detector". *Astroparticle Physics* 31.4 (2009), pp. 320–328. ISSN: 0927-6505. DOI: 10.1016/j.astropartphys.2009.03.002.

[2] K. Abe et al. "First gadolinium loading to Super-Kamiokande". *Nuclear Instruments and Methods in Physics Research Section A: Accelerators, Spectrometers, Detectors and Associated Equipment* 1027 (2022), p. 166248. ISSN: 0168-9002. DOI: 10.1016/j.nima.2021.166248.

[3] K. Scholberg. "Supernova neutrino detection". *Journal of Physics: Conference Series* 375.4 (July 2012), p. 042036. DOI: 10.1088/1742-6596/375/1/042036.

[4] K. Abe et al. "Measurement of the neutrino-oxygen neutral-current interaction cross section by observing nuclear deexcitation $\gamma$ rays". *Phys. Rev. D* 90 (7 Oct. 2014), p. 072012. DOI: 10.1103/PhysRevD.90.072012.

[5] L. Wan et al. "Measurement of the neutrino-oxygen neutral-current quasielastic cross section using atmospheric neutrinos at Super-Kamiokande". *Phys. Rev. D* 99 (3 Feb. 2019), p. 032005. DOI: 10.1103/PhysRevD.99.032005.

[6] K. Abe et al. "Measurement of neutrino and antineutrino neutral-current quasielasticlike interactions on oxygen by detecting nuclear deexcitation $\gamma$ rays". *Phys. Rev. D* 100 (11 Dec. 2019), p. 112009. DOI: 10.1103/PhysRevD.100.112009.

[7] S. Sakai et al. "Measurement of the neutrino-oxygen neutral-current quasielastic cross section using atmospheric neutrinos in the SK-Gd experiment" (Nov. 2023). arXiv: 2311.03842 [hep-ex].

[8] S. Agostinell et al. GEANT4 - *a simulation toolkit*. Nucl. Instr. Meth. A **506**:250–303 (2003).

[9] Y. Ashida. "Measurement of gamma-ray emission from neutron-$^{16}$O reactions with an 80 MeV quasi-mono energetic neutron beam". *PoS* NuFact2017 (2018), p. 077. DOI: 10.22323/1.295.0077.

[10] Y. Ashida. "Measurement of Neutrino and Antineutrino Neutral-Current Quasielastic-like Interactions and Applications to Supernova Relic Neutrino Searches". PhD thesis. Kyoto University, 2020. URL: https://inspirehep.net/literature/1787598.

[11] H. Kunxian. "Measurement of the Neutrino-Oxygen Neutral Current Quasi-elastic Interaction Cross-section by Observing Nuclear De-excitation $\gamma$-rays in the T2K Experiment". PhD thesis. Kyoto University, 2016. DOI: 10.14989/doctor.k19501. URL: https://repository.kulib.kyoto-u.ac.jp/dspace/bitstream/2433/215314/3/drigk04161.pdf.

[12] C. Petrone, M. Bacak, et al. "Exploring new frontiers of neutron inelastic cross section measurements at n_TOF: testing the performances of a mixed array of HPGe and LaBr3(Ce) detectors in beam". *CERN-INTC-2023-062; INTC-I-261* (2023). DOI: https://cds.cern.ch/record/2872407?ln=en.

[13] J. Allison et al. *Recent developemnts in* GEANT4. Nucl. Instr. Meth. A **835**:186-225 (2016).

[14] G. F. Knoll. *Radiation detection and measurement (1 1979)*. URL: https://www.osti.gov/biblio/6642801.

[15] J. Balibrea-Correa et al. "Pushing the high count rate limits of scintillation detectors for challenging neutron-capture experiments". *arXiv pre-print* (Nov. 2023). DOI: 10.48550/arXiv.2311.01365.

[16] X. Mao et al. "A high-energy gamma-ray source based on neutron capture". *"Nucl. Instr. Meth. A **835**:186-225 (2016)* 982 (2016), p. 164552. DOI: 10.1016/j.nima.2020.164552.

# Appendix

## DESCRIPTION OF THE PROPOSED EXPERIMENT

Please describe here below the main parts of your experimental set-up:

| Part of the experiment | Design and manufacturing |
|---|---|
| If relevant, write here the name of the fixed installation you will be using: $LaBr_3$ detectors present at the n_TOF installation | ☒ To be used without any modification<br>☐ To be modified |
| If relevant, describe here the name of the flexible/transported equipment you will bring to CERN from your Institute:<br>None | ☐ Standard equipment supplied by a manufacturer<br>☐ CERN/collaboration responsible for the design and/or manufacturing |

HAZARDS GENERATED BY THE EXPERIMENT

Additional hazard from flexible or transported equipment to the CERN site:

| Domain | Hazards/Hazardous Activities | | Description |
|---|---|---|---|
| Mechanical Safety | Pressure | ☐ | [pressure] [bar], [volume][l] |
| | Vacuum | ☐ | |
| | Machine tools | ☐ | |
| | Mechanical energy (moving parts) | ☐ | |
| | Hot/Cold surfaces | ☐ | |
| Cryogenic Safety | Cryogenic fluid | ☐ | [fluid] [m3] |
| Electrical Safety | Electrical equipment and installations | ☐ | [voltage] [V], [current] [A] |
| | High Voltage equipment | ☐ | [voltage] [V] |
| Chemical Safety | CMR (carcinogens, mutagens and toxic to reproduction) | ☐ | [fluid], [quantity] |
| | Toxic/Irritant | ☐ | [fluid], [quantity] |
| | Corrosive | ☐ | [fluid], [quantity] |
| | Oxidizing | ☐ | [fluid], [quantity] |
| | Flammable/Potentially explosive atmospheres | ☐ | [fluid], [quantity] |
| | Dangerous for the environment | ☐ | [fluid], [quantity] |
| Non-ionizing radiation Safety | Laser | ☐ | [laser], [class] |
| | UV light | ☐ | |
| | Magnetic field | ☐ | [magnetic field] [T] |
| Workplace | Excessive noise | ☐ | |
| | Working outside normal working hours | ☐ | |
| | Working at height (climbing platforms, etc.) | ☐ | |

| | | | |
|---|---|---|---|
| | Outdoor activities | ☐ | |
| Fire Safety | Ignition sources | ☐ | |
| | Combustible Materials | ☐ | |
| | Hot Work (e.g. welding, grinding) | ☐ | |
| Other hazards | | | |
| | | | |